BACTERIAL EXOPOLYSACCHARIDE-MEDIATED SYNTHESIS OF SILVER NANOPARTICLES AND THEIR APPLICATION ON BACTERIAL BIOFILMS

Adrianne Margaret Galvez, Kimberly Mae Ramos, Alexis Julianne Teja and Ronan Baculi*

Address(es):
Department of Biology, College of Science, University of the Philippines Baguio 1 Gov. Pack Road Baguio City 2600 Philippines.

*Corresponding author: rqbaculi@up.edu.ph

ABSTRACT

The development of multi-drug-resistant bacteria and their biofilm formation capabilities has decreased the effectiveness of antibiotics and other antimicrobial agents. Silver nanoparticle (AgNP) is currently being explored as an alternative strategy in countering biofilm-related infections. In this study, AgNP was biosynthesized using the extracted exopolysaccharide (EPS) from two obligate alkaliphilic bacteria, *Bacillus krulwichiae* M2.5 and *Bacillus cellulosilyticus* M4.1, isolated from a hyperalkaline spring in Zambales, Philippines. The samples exhibited an absorption peak at around 420 nm corresponding to the surface plasmon resonance of AgNPs as shown by UV-Vis analysis. The Fourier transform infrared (FTIR) spectroscopy spectra revealed functional groups in the EPS such as hydroxyl and carboxyl involved in the reduction of Ag^+ to AgNP. Scanning electron microscopy (SEM) coupled with energy dispersive X-ray (EDX) spectroscopy showed stable irregular and spherical AgNPs with an average size of 25.88 ± 10.49 nm and 23.99 ± 8.43 nm for *B. krulwichiae* M2.5 EPS-AgNP and *B. cellulosilyticus* M4.1 EPS-AgNP, respectively. The biosynthesized AgNPs significantly inhibited the biofilm formation of *Pseudomonas aeruginosa*, *Klebsiella pneumoniae* and *Staphylococcus aureus* in a dose-dependent manner as determined by microtiter plate assay. However, the results showed a reduced inhibitory effect of the synthesized AgNPs on established biofilms indicating the need for higher AgNP concentration. This study demonstrates that EPS from bacteria adapted to alkaline conditions can be used for efficient AgNP biosynthesis with potential biomedical applications.

Keywords: alkaliphilic bacteria, biofilm formation, anti-biofilm, exopolysaccharides, nanotechnology, silver nanoparticles

INTRODUCTION

In recent years, there has been a constant decrease in effectiveness of antibiotics mainly due to their unregulated use leading to the emergence of multi-drug-resistant bacterial strains and biofilm formation abilities. Many infections are caused by microorganisms growing in biofilms which are densely- packed communities of microbial cells surrounded with self-secreted matrix. Biofilm-related diseases are typically persistent infections characterized by slow development, resistance to host immune defenses and transient response to antimicrobial therapy. Therefore, it has become necessary to search for alternative healthcare approaches such as the utilization of nanomaterials to mitigate the problem of infections associated with bacterial biofilms (**Sanyasi *et al*., 2016**; **Mu *et al.,* 2016**).

Nanotechnology is an emerging field involving the synthesis and manipulation of nanoscale materials with anticipated applications in various fields. The increasing interest in nanoparticles lies on the premise of their unique optoelectronic and physico-chemical properties (**Kanmani and Lim, 2013**). Silver nanoparticle (AgNP) is the most commonly used nanoscale substance for various consumer products (**Saravanan and Nanda, 2010**). They have been used in many applications including food packaging, catheters, textiles, coatings, dental, pharmaceutics, medical therapeutics, and diagnosis (**Yoksan and Chirachanchai, 2010**). Silver ions have low toxicity toward animal cells but exhibit high toxicity toward bacterial and fungal cells (**Rauwel *et al*., 2015**). Several reports have successfully demonstrated that AgNPs have wide spectrum of inhibitory activity against many Gram-positive and Gram-negative bacteria, fungi and viruses (**Barapatre *et al.,* 2016**; **Duncan, 2011**; **Rauwel *et al.,* 2015**).

Currently, physical and chemical methods are commonly employed for the synthesis of AgNPs. Physical methods include evaporation-condensation as the most common approach in producing high concentration of relatively stable AgNPs (**Iravani *et al.,* 2014**). Meanwhile, chemical reduction of silver salt with the use of various reducing agents is the most commonly-used chemical method (**Ge *et al.,* 2014**). The synthesized nanoparticles are stable due to the capping

agents that protect them from agglomeration to surfaces (**Sato-Berŕu *et al*., 2009**). However, the above-mentioned methods have several disadvantages since they are costly, and involve high energy requirements and hazardous chemicals (**Sabri *et al*., 2016**). The increasing demand for eco-friendly and inexpensive approach in the synthesis of nanoparticles paved way for bio-based methods with the use of organisms, from prokaryotic bacteria to eukaryotic fungi and plants (**Iravani *et al.,* 2014**). Previous studies have demonstrated the synthesis of AgNPs using various polysaccharides including heparin (**Kemp *et al.,* 2009**), hyaluronic acid (**Liang *et al.,* 2015**), chitosan (**Wei *et al*., 2009**), cellulose (**Cheng *et al.,* 2013**), starch (**Mohanty *et al.,* 2012**) and alginate (**Mohan *et al.,* 2016**), however, most of these materials are unable to synthesize stable and monodispersed AgNPs. Polymers produced by microorganisms have been investigated for biogenic production of metal nanoparticles (**Kanmani and Lim, 2013**), specifically exopolysaccharides (EPS), which are biopolymers consisting of repeating units of sugar moieties joined by glycosidic linkages (**Mehta *et al.,* 2014**). Microbial EPS could serve as an efficient alternative substrate for metal nanoparticle production given their strong reducing and stabilizing properties largely contributed by their polyanionic functional groups (**Mehta *et al.,* 2014**). Apparently, microbial polysaccharides are of higher quality than plants and marine macroalgal polymers because of their novel functionality, stable cost and supply, and more reproducible production parameters (**Llamas *et al*., 2010**). Several species of lactic acid bacteria, such as those belonging to the genera *Lactobacillus, Pediococcus,* and *Enterococcus*, are known to produce EPS that could serve as reductant for AgNP synthesis (**Cioffi and Rai, 2012**).

Extremophilic microorganisms have developed adaptation strategies such as the synthesis of EPS which plays an important role in cell adhesion, retention of water, and concentration of nutrients under extreme conditions. The EPS from extremophiles offer potential biotechnological applications primarily due to their functional and structural diversity (**Nicolaus *et al.,* 2010**). The halophilic bacterium *Halomonas maura* has demonstrated the ability to produce mauran, a sulfated EPS used to stabilize gold nanoparticles (**Arias *et al.,* 2003**). Recently, the metal removal and reduction potential of an EPS from a psychrotrophic Arctic

soil bacterium *Pseudomonas* sp. was reported (**Sathiyanarayanan *et al.,* 2016**). However, the current knowledge on the structural and functional properties of EPS from alkaliphiles is still limited and so are their applications.

This study reports the production of EPS from two alkaliphilic bacterial strains isolated from hyperalkaline spring in Zambales, Philippines via enrichment cultures and subsequent application of the EPS for the synthesis of AgNPs. The biosynthesized AgNPs were further studied for their inhibitory effects against biofilm formation and established biofilms of bacterial pathogens namely *S. aureus, P. aeruginosa* and *K. pneumoniae*.

MATERIALS AND METHODS

Sample collection

Water samples were collected from Poon Bato hyperalkaline spring in Zambales, Philippines (15° 17' 22.5600" N, 120° 1' 28.2000" E). The samples were transferred aseptically into sterile bottles for analysis. The temperature, pH, dissolved oxygen, and conductivity of water were measured using water quality portable meter during the sample collection.

Isolation and screening of isolates for EPS production

Enrichment cultures were prepared by adding 10 mL of the collected water sample to 90 mL each of the broth media initially adjusted to pH 11 by the addition 1 M Na_2CO_3 (Table 1). The enrichment solutions were incubated at 37°C for 72 hours in a shaker incubator. Samples from the enrichment culture were serially diluted and were subsequently plated onto respective solid media. All plates were incubated at 37°C for 72 hours, and morphologically distinct colonies that grew on the plate were selected and purified via successive streak plating using the same solid media. EPS-producing bacteria were first selected on the basis of the mucoid appearance and ropiness by stroking them with sterile inoculating loop according to the method of **Kersani *et al.* (2017)**. Exopolysaccharide production of the isolates was further assessed by inoculation onto Congo red agar medium and incubation at 37°C for 48 hours. Positive result was indicated by the presence of black colonies with dry crystalline consistency (**Freeman *et al.,* 1989**). Pure cultures of EPS-producing isolates were maintained for further use in glycerol stock solutions (15% v/v).

Table 1 Growth media used in screening for EPS producing-alkaliphilic bacteria

Medium no.	Medium composition (L^{-1})
1	20 g glucose; 3.18 g KH_2PO_4; 5.2 g K_2HPO_4; 0.3 g $MgSO_4$; 5 g peptone; 0.6 g $(NH_4)_2SO_4$; 0.05 g $CaCl_2$; 0.2 mg $ZnSO_4$; 0.2 mg $CuSO_4$; 0.2 mg $MnSO_4$; 0.6 mg $FeSO_4$; 5 g yeast extract (**Dossounon *et al.,* 2016**)
2	5 g lactose; 5g tryptone; 5 g soya peptone; 5 g meat digest; 0.25 g $MgSO_4$; 0.5 g ascorbic acid; 19 g di-sodium glycerophosphate; 2.5 g yeast extract (**Kersani *et al.,* 2017**)
3	20 g glucose; 0.2 g $MgSO_4 \cdot 7H_2O$; 0.05 g $MnSO_4 \cdot 4 H_2O$; 8 g meat extract; 10 g peptone; 5 g $CH_3COONa \cdot 3 H_2O$; 2 g $C_6H_5Na_3O_7$; 4 g yeast extract; 2 g K_2HPO_4 (**Bajpai *et al.,* 2016**)
4	20 g sucrose; 0.2 g KH_2PO_4; 0.8 g K_2HPO_4; 0.2 g $MgSO_4 .7H_2O$; 0.1 g $CaSO_4.2H_2O$; 2.0 mg $FeCl_3$; Na_2MoO_4 .2H_2O (trace); 0.5 g yeast extract (**Mu'minah *et al.,* 2015**)
5	5 g peptic digest of animal tissue; 1 g yeast extract; 0.1 g $C_6H_5FeO_7$; 19.45 g NaCl; 8.8 g $MgCl_2$; 3.24 g Na_2SO_4; 1.8 g $CaCl_2$; 0.55 g KCl; 0.16 g $NaHCO_3$; 0.08 g KBr; 0.034 g $SrCl_2$; 0.022 g H_3BO_3; 0.004 g Na_2SiO_3; 0.0024 g NaF; 0.0016 g NH_4NO_3; 0.008 g Na_2HPO_4 (**Welman *et al.,* 2003**)

Phenotypic characterization of EPS-producing isolates

The isolates were examined for their Gram-reaction, endospore formation, and cultural characteristics, such as color, colony form, margin, surface, and elevation. Factors contributing to the optimum growth conditions of the bacterial isolates such as temperature, NaCl, pH and growth factor requirements were also determined. Determination of NaCl requirement of the isolates was performed using their respective solid media containing 1-15% NaCl concentrations. Growth of isolates on different pH (pH 7-12) was also assessed using the same media adjusted using 1 M Na_2CO_3. Plates for the temperature experiment were incubated at 4°C, 37°C, and 50°C for 24 hours. Growth factor requirements were determined following the method described by **Carino *et al*. (2017)**. Selected biochemical tests including hydrolysis of cellulose, starch, Tween 80, and gelatin; nitrate reduction, and activity of catalase, oxidase, protease and keratinase enzymes were also performed.

Sequencing and phylogenetic analysis of 16S rRNA genes of the isolates

Pure bacterial isolates were sent for amplification and sequencing of 16S rRNA gene to Macrogen Inc. Seoul, Korea. Amplification of 16S rRNA gene of the isolates was performed using the bacterial primers 27F (AGAGTTTGATCCTGGCTCAG) and 1492R (GGGTTACCTTGTTACGACTT) (**Lane, 1991**). Sequencing was carried out by using Big Dye terminator cycle sequencing kit v.3.1 (Applied Biosystems, USA). ChromasPro software (http://www.technelysium.com.au/) was used to manually evaluate the sequences and to remove low quality regions usually at the start and end of the fragment. DNA sequences were analyzed using the BLAST tool at the National Centre for Biotechnology Information (NCBI) server (http://blast.ncbi.nlm.nih.gov). The sequences were submitted for multiple alignments with reference sequences from the GenBank database using Clustal W. Phylogenetic tree was constructed with the Maximum Likelihood method based on the Tamura-Nei model of MEGA 7 software (**Tamura and Nei, 1993**) with evolutionary distances calculated according to Kimura's two-parameter correction method. The phylogenetic tree was evaluated through bootstrap analysis from 1000 bootstrap replicates. All sequences generated in this study were submitted to GenBank under accession numbers MH517429-MH517430.

Extraction and characterization of EPS from bacterial isolates

Exopolysaccharides produced by the isolates were extracted following the protocol described by **Kanmani *et al.* (2011)** with modifications. Briefly, isolates were grown in 200 mL of respective media broth and were incubated at 37°C for 18 hours. Subsequently, the broth cultures were heated to 100°C for 15 minutes to inactivate the EPS-degrading enzymes. The treated culture broths were then centrifuged at 6000 rpm for 10 minutes at 4°C. Double volumes of 95% ice cold ethanol was added to each supernatant and were maintained at 4°C overnight to complete the precipitation of EPS. Each mixture was then centrifuged at 12,000 rpm for 15 minutes, and the crude EPS was washed three times with sterile distilled water, air-dried, and kept at room temperature for characterization and AgNP synthesis. A solution for each EPS was prepared and was quantified by getting the concentration using phenol-sulfuric method (**Dubois *et al.,* 1956**). For the detection of functional groups on the extracted EPS, infrared spectra of each sample were recorded using Fourier transform infrared (FTIR) spectroscopy (Perkin-Elmer, Inc. USA) in the 4000-600 cm^{-1} with a resolution of 4 cm^{-1} and 16 scans.

Synthesis of silver nanoparticles using bacterial EPS

The crude EPS, amounting to 3 g for each isolate, was dissolved in 100 mL sterile distilled water at pH 9 to form a uniform dispersion. Then, 10 mM $AgNO_3$ was added to 3% EPS in a 1:1 ratio under stirring conditions, and the resulting solution was subsequently stored in a dark place at room temperature. After 24 hours incubation, the solutions were observed for the formation of yellow-brown color indicating the formation of AgNPs. The solutions were kept under incubation for 10 days to increase the concentration of the AgNPs. The nanoparticle synthesis was monitored by taking the OD within the range of 350-800 nm using UV-vis spectrophotometer (Jinan Hanon Instruments Co. Ltd. China) by withdrawing 3 mL of each sample every after two days of incubation. The resulting solutions were then repeatedly centrifuged at 12000 rpm for 20 minutes. The collected pellet was washed with 1 mL sterile distilled water, and then air-dried at room temperature for further analysis (**Saravanan *et al.,* 2017**; **Adebayo-Tayo and Popoola, 2017**; **Sirajunnisa *et al*., 2014**).

Characterization of silver nanoparticles

Synthesis of AgNPs using EPS by reduction of aqueous metal ions was monitored after 1, 3, 5, 7, and 10 days of incubation with the use of UV-Vis spectrophotometer (Jinan Hanon Instruments Co. Ltd. China) at wavelengths 350 to 800 nm with a resolution of 1 nm. Qualitative and quantitative analysis of the elemental composition of the synthesized nanoparticles were done using scanning electron microscopy (SEM) equipped with energy dispersive X-ray spectroscopy (EDX) (Horiba, Ltd. England). The samples were prepared by mounting a small amount of powdered AgNPs on the aluminum stub using a double-sided carbon tape. The analysis was performed at an accelerating voltage of 5 kV. The average particle size distributions of the AgNPs were calculated by averaging 200 particles from the SEM images using IMAGE J 1.46r software (NIH, USA). For further analysis on the synthesized AgNPs, a scan was performed within the two-theta angle in X-ray diffraction (XRD) (Shimadzu Maxima XRD 7000). For each sample, a thin

film of the powdered nanoparticles was mounted on a glass slide and the intensity peaks were recorded continuously with a Cu X-ray tube having voltage and current at 40 kV and 30 mA, respectively.

Anti-biofilm activity of the silver nanoparticles

To determine the efficacy of AgNPs in inhibiting biofilm formation, the microtiter plate assay was applied. The wells of sterile microtiter plate were filled with 100 μL overnight grown bacterial suspensions, *P. aeruginosa*, *S. aureus*, and *K. pneumoniae*, adjusted equivalent to 0.5 McFarland standard. Different concentrations of AgNPs (i.e 0.1, 0.5, 1, 5, 10, 25, and 50 μg/mL) were then added to the suspension and incubated overnight at 37ºC. After incubation, the medium was discarded and thoroughly washed with phosphate saline buffer (pH 7.2) to remove free-floating planktonic bacteria. Biofilms formed by bacteria adherent to the wells were fixed with sodium acetate (2% w/v) and were subsequently stained using 0.1% crystal violet dye for 30 minutes at 25ºC. Excess stain was rinsed off by thorough washing with sterile distilled water and plates were kept for drying. After which, 200 μL of 95% ethanol was added to the wells. To determine the efficacy of AgNPs in inhibiting established biofilm, each well of sterile microtiter plate was filled with 100 μL overnight grown bacterial suspensions and the plates were incubated for 24 hours. After incubation, the established biofilms in the plates were then added with 100 μL of different concentrations of AgNPs (i.e 0.1, 0.5, 1, 5, 10, 25, and 50 μg/mL) and incubated for another 24 hours at 37ºC. Similarly, biofilm mass was evaluated using crystal violet staining (**Barapatre et al., 2006**; **Kanmani et al., 2013**; **Rajkumari et al., 2017**; **Cho et al., 2013**). For quantification of the total biofilm formation, the absorbance was recorded at a wavelength of 570 nm. The percentage of biofilm inhibition was calculated using the equation:

$$\% \text{ biofilm inhibition} = [1 - (OD_{570} \text{ of cells with AgNPs} - OD_{570} \text{ of non-treated control}) \times 100]$$

Statistical analysis

All statistical analyses were performed using IBM Statistical Package for the Social Sciences (SPSS) version 20.0. For anti-biofilm activity, comparisons were carried out using univariate (uANOVA) or repeated measures analyses of variance (rANOVA) to evaluate the statistical significance at $P<0.05$. The experiments were done in triplicates and repeated two times.

RESULTS AND DISCUSSION

Isolation and identification of EPS-producing bacteria

Bacterial isolates were obtained from Poon Bato spring, a natural alkaline environment in the Zambales ophiolite complex of the Philippines. The sampling site is located downstream of the river which is rich in carbonate deposits. The average water temperature of the sampling site measured during collection was 28ºC and the measured pH was 11. Chemical analysis of the water samples revealed that calcium is the most abundant at 50.3 mg/L among the other components like magnesium, sulfate, chloride, and iron (Table 2). Poon Bato springs are typical $Ca^{2+}-OH^{-}$ type waters (**Barnes et al., 1967**) indicating that H_2 and CH_4 from regional serpentinization were incorporated. These serpentinization reactions result in both strongly alkaline and highly reducing circulating water in Poon Bato spring (**Cardace et al., 2015**).

Table 2 Physico-chemical characteristics of water samples obtained from Poon Bato Spring

PARAMETER	MEASUREMENT
pH	11
Temperature (˚C)	28
Conductivity (μS/cm)	781
Dissolved Oxygen (mg/L)	3.6
Calcium (mg/L)	50.3
Chloride (mg/L)	20.3
Sulfate (mg/L)	4.16
Magnesium (mg/L)	1.31
Iron (mg/L)	0.12
Nitrate (mg/L)	<LoD*
Manganese (mg/L)	ND**

*LoD — Limit of Detection (0.43 mg/L for nitrate), **ND — Not Detected

A total of sixteen bacterial isolates were obtained on the basis of mucoid property using enrichment media supplemented with different carbon source. Two isolates, M2.5 and M4.1, were selected for further study on the basis of high mucoid production and ropiness. Isolates M2.5 and M4.1 were grown in media supplemented with lactose and sucrose as carbon sources, respectively. Exopolysaccharide production of the isolates was further confirmed using the Congo red agar plate method. The isolates that tested positive for exopolysaccharide production exhibited black colonies with dry crystalline appearance. Based on phenotypic characterization (Table 3) and analysis of the 16S rRNA genes (Table 4), the isolates were identified as members of genus *Bacillus* under phylum Firmicutes. Specifically, isolates M2.5 and M4.1 showed 99% similarity to the obligate alkaliphiles *Bacillus krulwichiae* and *Bacillus cellulosilyticus* strains, respectively. A phylogenetic analysis confirmed their similarity to the respective species (Figure 1).

Table 3 Phenotypic characteristics of the alkaliphilic bacterial strains from Poon Bato spring

Characteristics	Isolate M2.5	Isolate M4.1	Characteristics	Isolate M2.5	Isolate M4.1
Cultural characteristics (color, colony form, margin, surface, elevation)	white, circular, entire, smooth, raised	cream, circular, entire, smooth, raised	Temperature requirement:		
			4˚C	-	-
			37˚C	+	+
			50˚C	-	-
			NaCl requirement:		
Gram reaction	G+	G+	10%	+	-
Cell morphology	rod	rod	11%	+	-
Endospore location	ST	ST	12%	+	-
			13%	+	-
			14%	+	-
			15%	+	-
Production of:					
Cellulase	-	-	pH tolerance: (pH_optimum)	(9-12) 11	(9-12) 11
Amylase	+	+			
Lipase	+	+			
Gelatinase	+	+			
Nitrate reductase	+	+	Growth factor requirement:		
Catalase	+	+	dextrose	+	+
Oxidase	+	+	yeast extract	+	+
Protease	+	+			
Keratinase	-	-			

*ST, subterminal; +, positive/with growth; -, negative/ without growth; G+, Gram-positive.

Table 4 Phylogenetic affiliations of the alkaliphilic bacterial isolates from Poon Bato Spring

Isolate	Nearest phylogenetic affiliation	Accession number of the nearest phylogenetic affiliation	% Similarity	Phylogenetic group
M2.5	*Bacillus krulwichiae*	NR_114066.1	99%	Firmicutes
M4.1	*Bacillus cellulosilyticus*	NR_074904.1	99%	Firmicutes
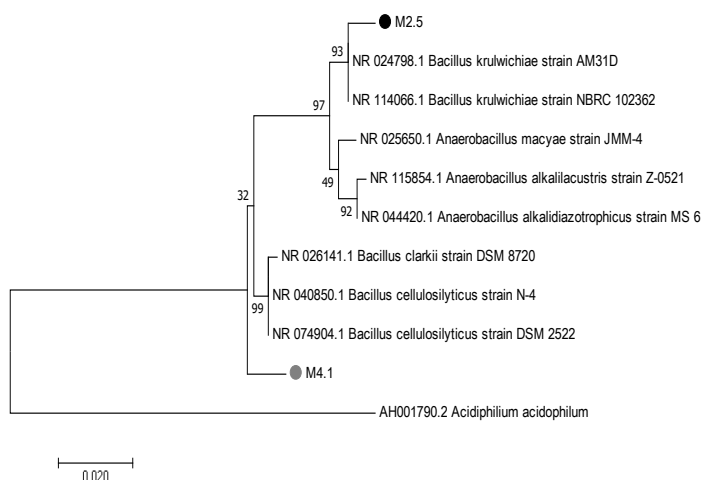
Figure 1 Phylogenetic tree based on 16S rRNA gene sequences highlighting the phylogenetic position of the two isolates relative to other alkaliphilic strains. *Acidiphilium acidophilum* was used as outgroup. The evolutionary history was inferred by using the Maximum Likelihood method based on the Tamura-Nei model. The tree is drawn to scale, with branch lengths measured in the number of substitutions per site. The analysis involved 18 nucleotide sequences. Evolutionary analyses were conducted in MEGA7.

The type of carbon source added to the screening media is important on EPS production because it serves as a source of energy for production and secretion of EPS (**Mu'minah et al., 2015**). Likewise, **Grobben et al. (1996)** reported that the regulation of the EPS biosynthetic pathway in *L. bulgaricus* NCFB 2772 could be dependent on the carbohydrate source. Utilization of lactose as a carbon source was reported by **Yuksekdag and Aslim (2008)** to produce high amount of EPS as compared to when other sugar carbon sources were used. Similarly, **Emtiazi et al. (2004)** noted that two strains of *Azobacter* species were able to produce maximum amount of EPS with sucrose as the carbon source. This is due to the direct link of carbon sources to cell proliferation and metabolite biosynthesis which can regulate secondary metabolism through catabolic repression (**Khani et al., 2016**).

The phylum Firmicutes consists mostly of Gram-positive bacteria which are phenotypically and physiologically diverse allowing them to inhabit a wide variety of environments including hypersaline and hyperalkaline habitats. Members of this phylum have been reported in several bacterial diversity studies of alkaline environments such as the Lonar lake in India (**Joshi et al., 2008**), the Cabeco de Vide aquifer in Portugal (**Tiago et al., 2004**), the Cedars in California (**Brazelton et al., 2013**), and the Manleluag hyperalkaline spring in the Philippines (**Baculi et al., 2015**) where they made up a large portion of the total isolates collected. The high occurrence of *Bacillus* species in alkaline saline environments may be due to their nutritional versatility, stress-tolerant thick-walled endospores, and broad tolerance for environmental extremes. The presence of both strains in alkaline environments has been previously documented in Lonar Lake in India. Isolate M2.5 was closely affiliated to obligate alkaliphilic, halotolerant *Bacillus krulwichiae strain,* isolated from Lonar Lake and alkaline soil in Japan (**Tambekar and Dhundale, 2012**). Meanwhile, isolate M4.1 was closely affiliated to *Bacillus cellulosilyticus* DSM 2522ᵀ previously isolated in Japan with pH tolerance of 8-10 and growth temperature range of 20-40°C (**Vishnuvardhan Reddy et al., 2015**). Hence, it can be inferred that the alkaline pH of Poon Bato spring could possibly support the growth of these bacteria. The occurrence of EPS-producing *Bacillus* strains has been previously documented such as *B. licheniformis* and *B. subtilis* (**Berekaa, 2014**; **Abdul Razack et al., 2013**). In this study, the ability of the alkaliphilic isolates closely related to *B. krulwichiae* and *B. cellulosilyticus* to produce EPS has not yet been reported.

Characterization of EPS produced by the isolates

Based on the analysis, *B. cellulosilyticus* M4.1 has produced 124.5 mg/mL crude EPS when inoculated into sucrose-rich medium. Meanwhile, the *B. krulwichiae* M2.5 secreted 67.67 mg/mL crude EPS lactose as carbon source. The FTIR spectra of the crude EPS produced by the two strains revealed characteristic functional

groups, such as a broad-stretching hydroxyl group at 3443 cm⁻¹ and 3190 cm⁻¹, C-H stretching peak at 3072 cm⁻¹ and 2889 cm⁻¹, and C=O stretching peak of Amide I and carboxyl groups at 1685 cm⁻¹ and 1684 cm⁻¹ (Figure 2).The hydroxyl stretching vibration of the polysaccharide correlates to the carbohydrate ring and is responsible for the characteristic water solubility of the EPS (**Karbowiak et al., 2007**). The observed C-H stretching vibration usually corresponds to hexoses, like glucose or galactose (**Castellane et al., 2015**). The presence of carboxyl and hydroxyl groups in the EPS may serve as binding sites for divalent cations (**Bramhachari and Dubey, 2006**). The differences in the peaks at 1300 – 900 cm⁻¹ which corresponds to the fingerprint region of the spectrum unique for every molecular species, suggest possible chemical differences between the EPS produced by the two strains. Taken all together, the FTIR spectra of the extracted EPS revealed the heteropolymeric nature of the sample due to the presence of different functional groups which are powerful reducing agents and they may be accountable for the bio-reduction of Ag⁺ ions leading to Ag⁰ nanoparticle synthesis.
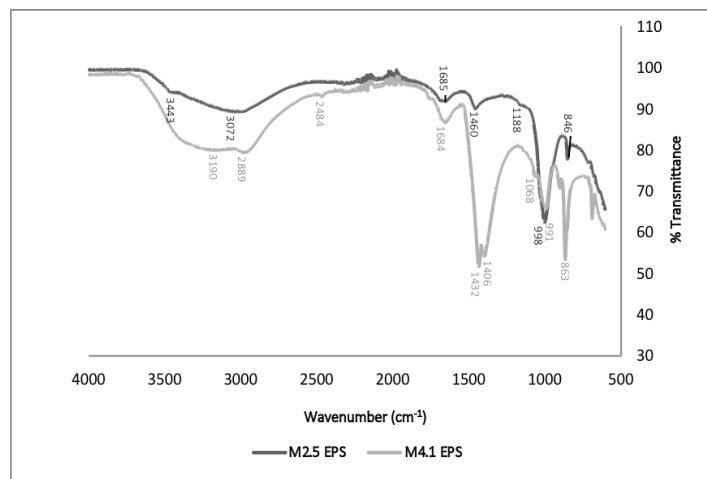
Figure 2 FTIR spectra of exopolysaccharide extracted from *B. krulwichiae* M2.5 and *B. cellulosilyticus* M4.1.

Biosynthesis and UV-Vis characterization of silver nanoparticles

The formation of AgNPs by reduction of Ag⁺ to Ag⁰ was observed after the addition of EPS in a solution of silver nitrate, followed by incubation at room temperature in the dark. Biosynthesis of AgNPs was evident based on the color change of individual reaction mixture from colorless to yellowish brown immediately upon the addition of EPS. The maximum color intensity was attained as brown after 24 hours and remained stable throughout the 10-day storage period. No color change was observed in the control solutions containing only AgNO₃ that was incubated at the same condition as the experimental set-ups (Figure 3). AgNPs are known to exhibit a range of colors due to their surface plasmon resonance (SPR) and can be characterized accordingly by measurement of the absorption at different wavelengths (**Chhatre et al., 2012**). The resulting color of the solutions suggests possible details in the size and shape of the nanoparticles produced. As the particle size decreases, the SPR shifts to a shorter wavelength resulting to the absorption of blue light. The green and red lights are then scattered off a white background, thereby resulting to a yellow to brown color. Furthermore, **Logaranjan et al. (2016)** stated that the appearance of yellow-colored reaction mixture indicates the formation of spherical shaped AgNP, which corroborates the SEM results in this experiment.

The visual observations were confirmed using UV-Vis spectroscopy by measuring the surface plasmon resonance (SPR) peaks for both sample solutions. AgNPs usually reveal such unique and tunable optical properties due to their strong SPR transition that are dependent on factors such as shape and size (**Hebeish et al., 2012**). For both samples, an intense absorption peak was noted around 420 nm with a broad band (Figure 4), which indicates the formation of AgNPs in varying sizes (**Kanmani and Lim, 2013**). No characteristic absorption of AgNPs was observed in the solution containing only AgNO₃. **Kalimuthu et al. (2008)** reported that observation of this peak, assigned to a surface plasmon, is well-documented for various metal nanoparticles with sizes ranging from 2 nm to 100 nm. In the

experiment, the intensity of the absorption maximum increased with longer incubation time.

Exopolysaccharide structures are known to exhibit excess negatively-charged functional groups which allow them to attract metal cations (**Sathiyanarayanan et al., 2016**). This polyanionic nature of EPS is confirmed by the FTIR results presented in this study. The reduction of AgNO$_3$ possibly involved the formation of electrostatic interactions between the positively charged silver ions and the negatively charged EPS molecules (**Mariselvam et al., 2014**). This interaction confines the free electrons of the nanoparticles resulting to a high free electron density, hence the observance of SPR peak at lower wavelength (**Razack et al., 2016**).
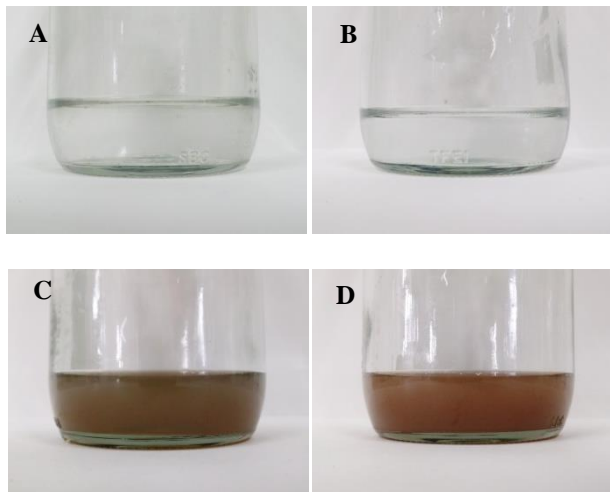
Figure 3. EPS-AgNO$_3$ reaction mixtures showing (A-B) colorless control solutions, and (C-D) brown colored solutions attained after 24 hours using EPS extracted from *B. krulwichiae* M2.5 and *B. cellulosilyticus* M4.1, respectively.
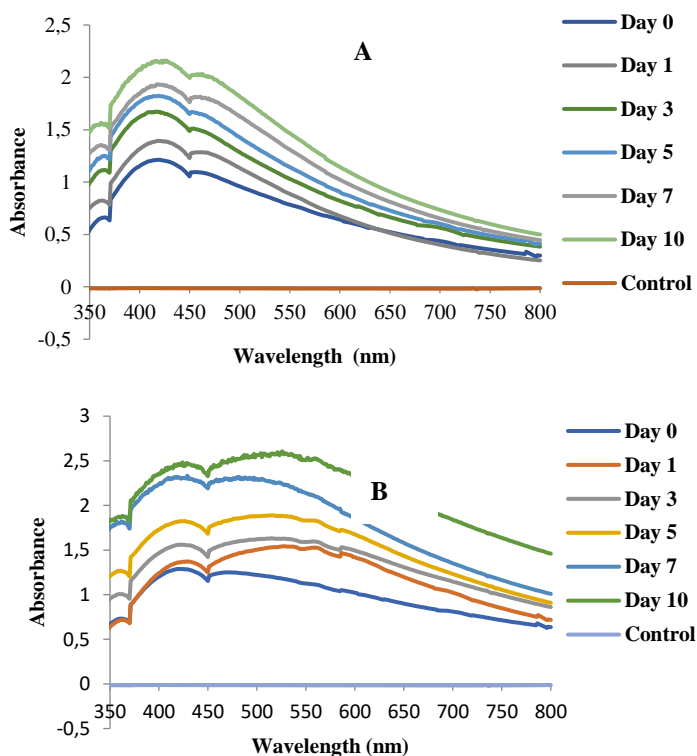
Figure 4 UV-Vis absorption spectra indicating the synthesis of AgNPs using EPS from (A) *B. krulwichiae* M2.5 and (B) *B. cellulosilyticus* M4.1 during different incubation period. The peak was noted around wavelength 420 nm for both sample solutions.

Fourier-transform infrared (FTIR) analysis of silver nanoparticles

The FTIR spectrum measurement was carried out to identify the possible functional groups of EPS responsible for the bio-reduction of Ag$^+$ and stabilization of the AgNPs. The FTIR spectrum of the AgNPs revealed various characteristic

peaks ranging from 3398 to 604 cm^{-1} and from 3320 to 603 cm^{-1} in *B. krulwichiae* M2.5 and *B. cellulosilyticus* M4.1, respectively (Figure 5). A broad and weak absorption peak for both AgNPs was observed at 3398 cm^{-1} and 3320 cm^{-1} for stretching vibration of the hydroxyl groups (OH), peak at 2958 cm^{-1} corresponded to CH stretching of aldehyde and peaks at 1764 cm^{-1} and 1753 cm^{-1} could be due to C=O stretch of saturated esters. The absorption peaks at 1684 cm^{-1} and 1652 cm^{-1} for both AgNPs indicated the presence of C=O stretching of the amide or carboxyl group while peaks at 947 cm^{-1} and 945 cm^{-1} correspond to the C-H, C-C, and C-OH ring and side group vibration of carbohydrates (Figure 5). Most of the peaks observed in the FTIR spectrum of EPS-stabilized AgNPs differed from the FTIR spectrum results of the crude EPS. Once the EPS reacted with silver in the solution, the bands shifted in peaks due to possible interaction of silver with the functional groups in the EPS. In addition, the absorption of the characteristic ß-glycosidic linkages at 998 cm^{-1} and 991 cm^{-1} respectively was absent in the FTIR spectra of the AgNPs formed, indicating probable involvement of this linkage towards formation of AgNP (**Mehta et al., 2014**). The functional groups observed such as aldehyde, hydroxyl, carboxyl, and esters could have been responsible for the reduction and stabilization of AgNPs as previously reported (**Adebayo-Tayo and Popoola, 2017**). The observed changes both in the positions and in the strengths of the FTIR spectra suggest a strong interaction of Ag^0 with the EPS functional groups.
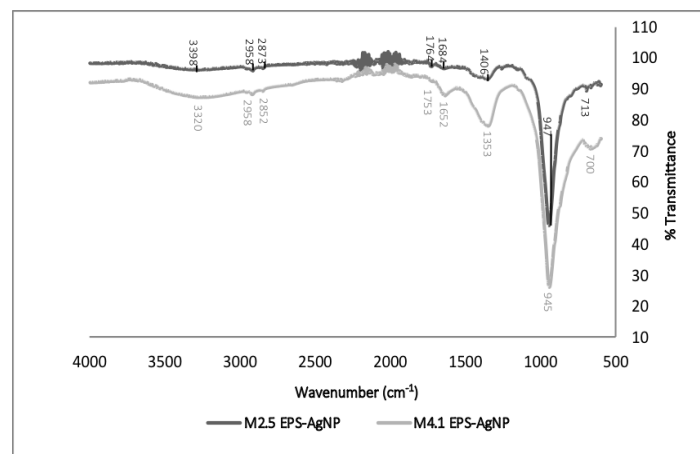
Figure 5 FTIR spectra of silver nanoparticles synthesized using exopolysaccharide extracted from *B. krulwichiae* M2.5 and *B. cellulosilyticus* M4.1.

Scanning electron microscopy (SEM) analysis of silver nanoparticles

It is evident that the synthesized AgNPs using the EPS from *B. krulwichiae* M2.5 have irregular and spherical shapes with size ranging from 7-61 nm and average size of 25.88± 10.49 nm. On the other hand, the AgNPs obtained using the EPS from *B. cellulosilyticus* M4.1 displayed the same morphology, with size ranging from 8-58 nm and average size of 23.99± 8.43 nm (Figures 6 and 7). The observed small particle size, and characteristic shape were almost similar to the results of **Phanjom and Ahmed (2017)** who demonstrated the synthesis of spherical and irregular-shaped AgNPs of size 5-13 nm at alkaline pH of 9 using filtrate of *Aspergillus oryzae*. The authors also reported that the size of the particles decreases with increasing pH and were found to be more uniform in sizes with almost spherical in shape. Similar observations were previously reported where alkaline condition was found to be effective for rapid reduction of metal ions by *Coriolus versicolor* (**Sanghi and Vermi, 2009**) and *Escherichia coli* (**Gurunathan et al., 2009**). The synthesis of smaller size AgNPs at alkaline condition can be explained by the reduction of silver ions by electrons provided by OH$^-$ ions. The present results validated the plasmon resonance peak obtained using UV-Vis analysis. The plasmon resonance peak of AgNPs is usually detected at shorter wavelength region at higher pH with a concomitant decrease in the size of the AgNPs (**Alqadi et al., 2014**).The synthesized nanoparticles appreciably aggregated as clusters due to extremely small dimensions. Moreover, agglomeration of AgNPs can be due to the high surface energy and high surface tension of the ultrafine nanoparticles ranging from 1-100 nm in diameter (**Agrawal and Kulkarni, 2017**).
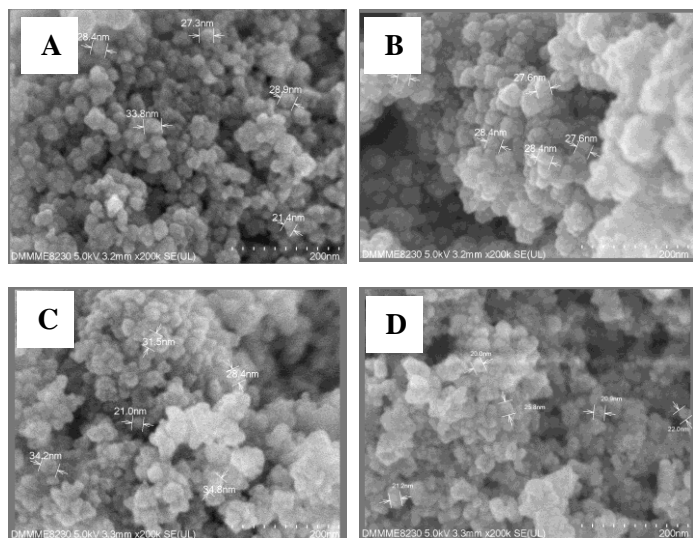
Figure 6 SEM images showing the size and morphology of the AgNPs synthesized using the exopolysaccharide of (A-B) *Bacillus krulwichiae* M2.5 and (C-D) *Bacillus cellulosilyticus* M4.1.
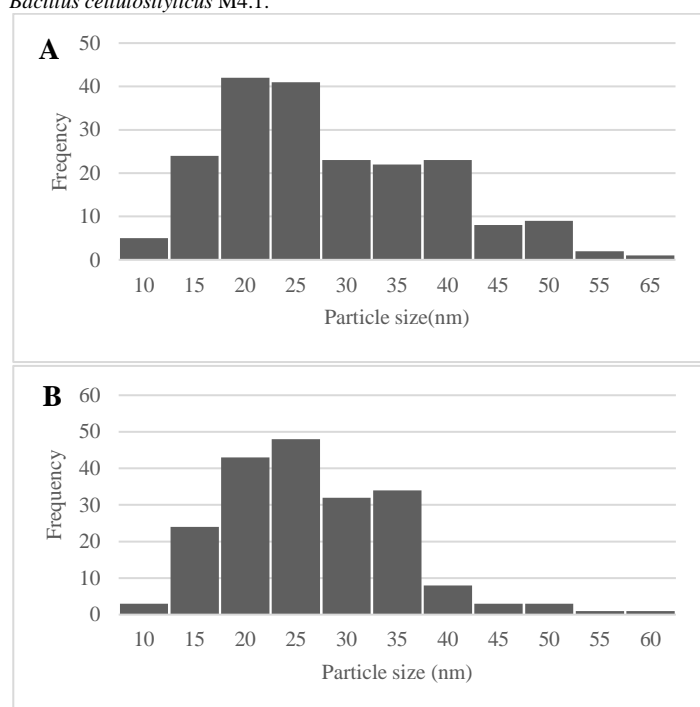
Figure 7 Particle size distribution of AgNPs synthesized using EPS from (A) *B. krulwichiae* M2.5 and (B) *B. cellulosilyticus* M4.1.

Energy dispersive x-ray (EDX) analysis of silver nanoparticles

The EDX profiles of the biosynthesized AgNPs showed the presence of strong peaks for elemental silver along with trace peaks for other elements (Figure 8). The characteristic optical absorption peak at 3 keV is typical for metallic silver nanocrystallites due to their surface plasmon resonance (**Gomaa, 2016**). The presence of peaks specific for C, N and O could be due to cellular components including proteins and carbohydrates that possibly acted as stabilizing or capping agents in the formation of AgNPs. This is consistent with the results of the FTIR analysis which revealed the possible presence of functional groups involved in stabilization of synthesized nanoparticles. The AgNPs synthesized from the EPS of *B. krulwichiae* M2.5 and *B. cellulosilyticus* M4.1 are composed of 72.35% and 81.07% Ag, respectively. The difference in percent Ag content can be accounted to the differences in EPS composition. It was reported that the use of low molecular weight protein-rich EPS led to the production of AgNPs with higher Ag content (**Jian *et al.*, 2016**).
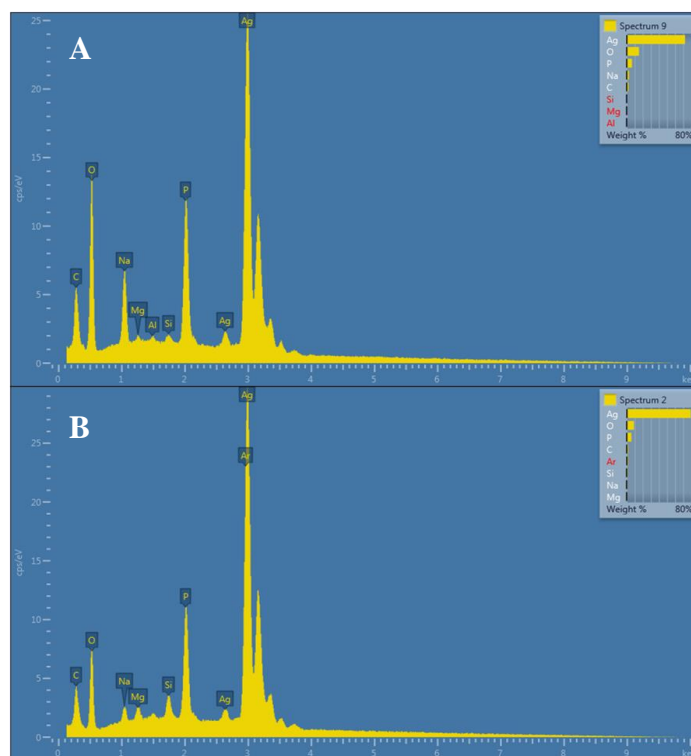
Figure 8 EDX spectra of silver nanoparticles synthesized using EPS extracted from (a) *Bacillus krulwichiae* M2.5 and (b) *Bacillus cellulosilyticus* M4.1.

X-ray diffraction (XRD) analysis of silver nanoparticles

X-ray diffraction measurements were carried out to study the crystallinity and the preferential orientation of the synthesized AgNPs. The XRD spectra exhibited 9 sharp diffraction lines for both AgNPs synthesized using EPS from *B. krulwichiae* M2.5 and *B. cellulosilyticus* M4.1 (Figure 9). These diffraction peaks existed at low angles of 2θ ranging from 3° to 80° and indicate the crystal planes of the sample AgNPS. The presence of peaks on the first sample at 2θ values 20.82°, 29.6°, 33.5°, 36.64°, 47.78°, 54.92°, 57.5°, 71.92° and 87.42° correspond to respective d-spacing (100), (110), (111), (210), (211), (211), (211), (310), and (320) (Figure 9a), while XRD peaks on the second sample at 2θ values 19.56°, 20.78°, 30.22°, 33.72°, 36.58°, 43.16°, 48.5°, 55.24°, and 60.66° correspond to (100), (100), (110), (111), (200), (110), (110), (110), and (110) planes, respectively (Figure 9b). The typical Ag diffraction peaks obtained imply the presence of a face-centered cubic (FCC) structure on the crystalline nanoparticles (**Kanmani and Lim, 2013**). These findings thereby support the idea of EPS-Ag ion interaction leading to AgNP stabilization.
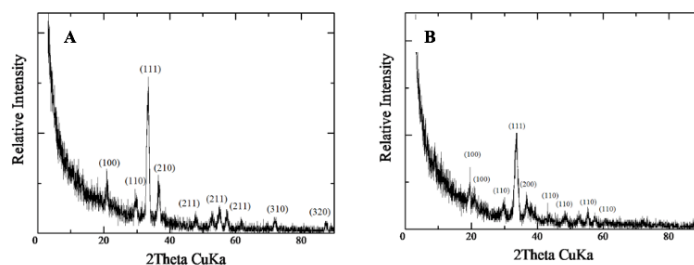
Figure 9 XRD pattern of synthesized AgNPs after 10-day incubation by EPS from (a) *Bacillus krulwichiae* M2.5 and (b) *Bacillus cellulosilyticus* M4.1.

Anti-biofilm activity of silver nanoparticles

Considering the important role of biofilms in infectious diseases, there has been an increased effort towards the development of AgNPs that will modulate the formation of bacterial biofilms. In the current study, the effect of EPS-AgNPs was evaluated on the biofilm formation and established biofilms of Gram-negative bacteria, *P. aeruginosa* and *K. pneumoniae*, and Gram-positive bacterium, *S. aureus*.

To explore the efficacy of different concentrations of the synthesized AgNPs against biofilm formation, planktonic cells of *P. aeruginosa*, *K. pneumoniae*, and *S. aureus* were added in 96-well plate in the presence of varying AgNP concentrations (0.1, 0.5, 1, 5, 10, 25, and 50 μg/mL). The results showed that the

biosynthesized AgNPs significantly reduced ($P \leq 0.05$) the formation of biofilms for all the tested bacterial strains at increasing AgNP concentrations. The highest concentration of AgNPs used (50 µg/mL) gave percent inhibition of 54.65% and 71.12% on *P. aeruginosa*, 42.25% and 70.05% on *K. pneumoniae*, and 49.90% and 65.25% on *S. aureus*, for *B. krulwichiae* M2.5 EPS-AgNP and *B. cellulosilyticus* M4.1 EPS-AgNP, respectively. Notably, all other concentrations showed significant reduction in *P. aeruginosa* biofilm even at the lowest concentration used. However, biofilm inhibition in *K. pneumoniae* and *S. aureus* was observed at higher AgNP concentrations (≥ 5 µg/mL), which could be correlated to the decreased susceptibility of the strains to the AgNPs. In terms of effectiveness of the AgNPs in biofilm inhibition, no significant differences were observed between 0.1- 10 µg/mL concentrations (Figure 10). The production of EPS is an important hallmark of bacterial biofilms which is crucial for the initial attachment of the cells as well as for holding the cells together. The AgNPs could possibly be involved in neutralizing this adhesive substance needed for biofilm formation (**Chaudhari et al., 2012**). It has been reported that AgNPs could penetrate and accumulate in bacterial cytoplasm once adhered in the cell membrane. The accumulated AgNPs could then inactivate enzymes through coagulation with sulfur- and phosphorus-containing compounds such as those present in proteins responsible for EPS synthesis (**Matsukawa and Greenberg, 2004**).
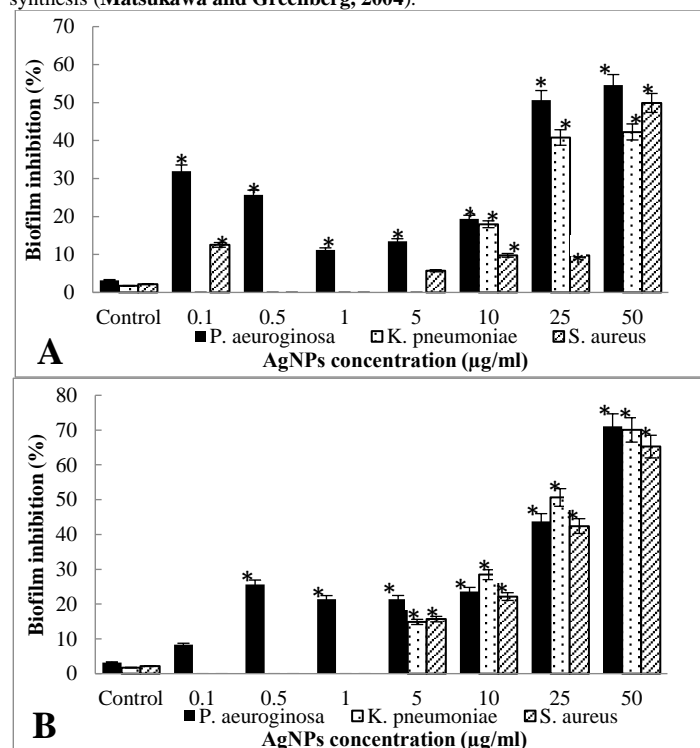
Figure 10 Effect of different concentrations of (a) *B. krulwichiae* M2.5 EPS-AgNPs and (b) *B. cellulosilyticus* M4.1 EPS-AgNPs on biofilm formation of *P. aeruginosa*, *K. pneumoniae*, and *S. aureus*. The experiment was performed in triplicate and repeated two times. Bars represent standard deviation and * denotes P-value (P<0.05).

Mature biofilms are characterized by high tolerance to antimicrobial agents which is largely contributed by altered growth rate of the cells and the rise of resistant sub-populations. The efficacy of the synthesized AgNPs against established biofilms was assessed by treating 24-hour culture of the test strains with varying AgNP concentrations (0.1, 0.5, 1, 5, 10, 25, and 50 µg/mL). The results showed a reduced inhibitory effect of the synthesized AgNPs on established biofilms as compared to its effect on biofilm formation. At the maximum concentration used (50µg/mL), the percent inhibitions were 26.55% and 58.34% on *P. aeruginosa* and 53.23% and 60.60% on *K. pneumoniae* using *B. krulwichiae* M2.5-AgNP and *B. cellulosilyticus* M4.1-AgNP, respectively. No inhibition was evident on the biofilm mass of *S. aureus* treated with 0.1 to 25 µg/mL AgNP concentrations, however, 2.22% inhibition was observed at 50µg/mL (Figure 11), indicating that higher concentration of AgNP is necessary to significantly inhibit the established biofilms of *S. aureus*. It has been reported that the effect of AgNPs on the removal of biofilms appears to be size-dependent which is important in modulating their transport within biofilms with their self-diffusion coefficients decreasing with increasing size (**Peulen and Wilkinson, 2011**). **Loo et al. (2013)** reported that smaller nanoparticles are more effective in reducing biofilms because they have higher surface area that translates to a higher availability of surface area for oxidation, and therefore Ag⁺ release. Due to their minute size, AgNPs can possibly reach the colonies inside the biofilm and attach to the surface of the cell membrane disturbing its permeability and respiration (**Loo et al., 2013**; **Gurunathan et al.,**

2014). The present work demonstrated the synthesis of AgNPs with size ranging from 11-61 nm and complete detachment of established biofilms was not achieved even at the highest concentration used. This observation is similar to the report of Loo et al. (2013) which showed that AgNPs which are approximately 20 nm and 35 nm diameters have 75% inhibition. Moreover, their results showed that AgNPs with 8 nm diameter were most effective in reducing *P. aeruginosa* biofilm, which accounted for 90% inhibition. The low anti-biofilm activity of the synthesized AgNPs against established biofilms in our study might be due to the aggregation of the nanoparticles as revealed by SEM analysis. The potential application of AgNPs against biofilms becomes limited when they tend to aggregate into larger structures during post-synthesis phase (**Sanyasi et al., 2016**). Biofilms are characterized by the presence of water channels or pores within the matrix that serve as nutrient transport channels. Aggregation into larger clusters thereby limits the penetration and dispersion of AgNPs within the biofilm matrix (**Loo et al., 2013**). Taken together, the results indicated that the synthesized AgNPs using EPS were more effective in inhibiting biofilm formation than in established biofilms of *P. aeruginosa*, *K. pneumoniae*, and *S. aureus*. Hence, they could be used in the development of potential anti-biofilm and antimicrobial agents for various biomedical applications. However, further studies are needed to investigate the mechanism of AgNPs against pathogenic bacterial biofilms.
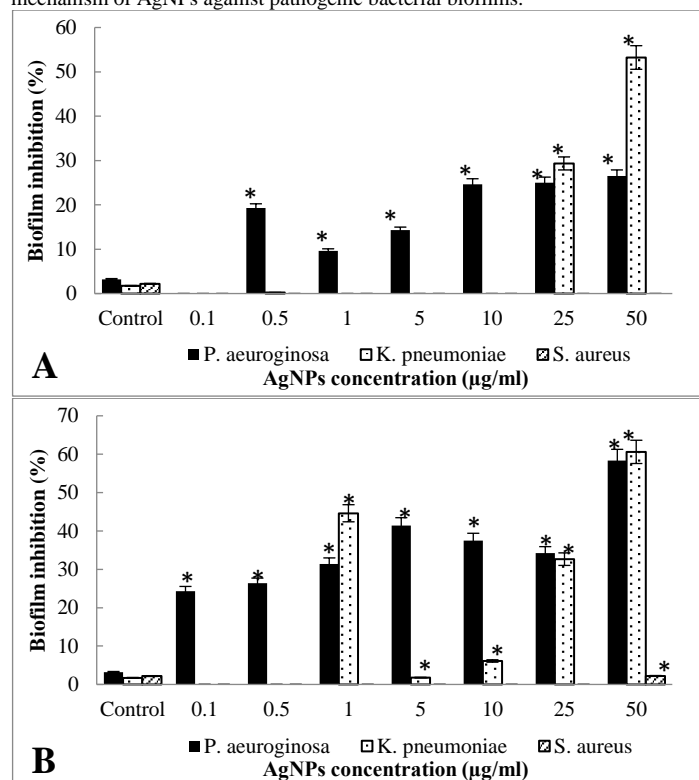
Figure 11 Effect of different concentrations of (a) *B. krulwichiae* M2.5 EPS-AgNPs and (b) *B. cellulosilyticus* M4.1 EPS-AgNPs on established biofilm of *P. aeruginosa*, *K. pneumoniae*, and *S. aureus*. The experiment was performed in triplicate and repeated two times. Bars represent standard deviation and * denotes P-value (P<0.05).

CONCLUSION

This study demonstrates the biosynthesis of AgNPs using the EPS of the alkaliphilic bacteria, *Bacillus krulwichiae* M2.5 and *Bacillus cellulosilyticus* M4.1, by effectively acting as reducing and stabilizing agents. Both of the extracted EPS from the two isolates were able to reduce the Ag⁺ ions from AgNO₃ and synthesize stable AgNPs. Notably, the biosynthesized AgNPs were able to significantly inhibit ($P \leq 0.05$) biofilm formation at increasing AgNP concentrations in all bacterial strains used, namely *P. aeruginosa*, *K. pneumoniae*, and *S. aureus*. However, the synthesized AgNPs were observed to have reduced inhibitory activity on established biofilms suggesting the need for higher concentrations of AgNPs. Further, the underlying mechanism of inhibition of AgNPs in biofilm formation should be investigated by determining the exact mode of action of AgNPs on bacterial biofilms.

REFERENCES

ABDUL RAZACK, S., VELAYUTHAM, V., THANGAVELU, V. 2013. Medium optimization for the production of exopolysaccharide by *Bacillus subtilis* using synthetic sources and agro-wastes. *Turkish J Biol,* 37: 280-288. https://dx.doi.org/10.3906/biy-1206-50

ADEBAYO-TAYO, B., POPOOLA, A.O. 2017. Biogenic synthesis and antimicrobial activity of silver nanoparticle using exopolysaccharides from lactic acid bacteria. *Int J Nano Dimens,* 8(1): 61-69. https://dx.doi.org/10.22034/ijnd.2017.24377

AGRAWAL, P.N., KULKARNI, N.S. 2017. Biosynthesis and characterization of silver nanoparticles. *Int J Curr Microbiol Appl Sci,* 6(4): 938-947. https://dx.doi.org/10.20546/ijcmas.2017.604.118

ALQADI, M.K., ABO NOGTAH , O.A., ALZOUBI, F.Y. 2014. pH effect on the aggregation of silver nanoparticles synthesized by chemical reduction. *Mater Sci-Poland* 32(1): 107-111. https://dx.doi.org/10.2478/s13536-013-0166-9

ANSARI, S., NEPAL, H.P., GAUTAM, R., SHRESTHA, S., NEOPANE, P., GURUNG, G. 2015. Community acquired multi-drug resistant clinical isolates of *Escherichia coli* in a tertiary care center of Nepal. *Antimicrob Resist Infect Control,* 4:15.; https://dx.doi.org/10.1186/s13756-015-0059-2

ARIAS, S., DEL MORAL, A., FERRER, M.R., TALLON, R., QUESADA, E., BEJAR, V. 2003. Mauran, an exopolysaccharide produced by the halophilic bacterium *Halomonas maura*, with a novel composition and interesting properties for biotechnology. *Extremophiles*, 7: 319–326. https://dx.doi.org/10.1007/s00792-003-0325-8

BACULI, R.Q., LANTICAN, N.B., DE LOS REYES III, F.L., RAYMUNDO, A.K. 2015. Prokaryotic community analysis of a hyperalkaline spring in the Philippines using 16S rRNA gene clone library construction. *Philip J Sci*, 144(1): 1-12.

BAJPAI, V.K., RATHER, I.A., MAJUMDER, R., SHUKLA, S., AERON, A., KIM, K., PARK, Y.H. 2016. Exopolysaccharide and lactic acid bacteria: perception, functionality and prospects. *Bangladesh J Pharmacol, 11*(1): 1-23. https://dx.doi.org/10.3329/bjp.v11i1.23819

BARAPATRE, A., AADIL, K., JHA, H. 2016. Synergistic antibacterial and antibiofilm activity of silver nanoparticles biosynthesized by lignin-degrading fungus. *Bioresour Bioprocess*, 3(8). https://dx.doi.org/10.1186/s40643-016-0083-y

BARNES, I., LAMARCHE, V.C., HIMMELBE, G. 1967. Geochemical evidence of present-day serpentinization. *Science*, 156: 830–832. https://dx.doi.org/10.1126/science.156.3776.830

BEREKAA, M. 2014. Improved exopolysaccharide production by *Bacillus licheniformis* strain-QS5 and application of statistical experimental design. *Int J Curr Microbiol App Sci*, 3(4): 876-886.

BRAMHACHARI, P., DUBEY, S. 2006. Isolation and characterization of exopolysaccharide produced by *Vibrio harveyi* strain VB23. *Lett Appl Microbiol*, 43: 571–577. https://dx.doi.org/10.1111/j.1472-765X.2006.01967.x

BRAZELTON, W., MORRILL, P., SZPONAR, N., SCHRENK, M. 2013. Bacterial communities associated with subsurface geochemical processes in continental serpentinite springs. *J Appl Environ Microbiol*, 79(13): 3906–16. https://dx.doi.org/10.1128/AEM.00330-13

CARDACE, D., MEYER-DOMBARD, D.R., WOYCHEESE, K., ARCILLA, C.A. 2015. Feasible metabolic schema associated with high pH springs in the Philippines. *Front Microbiol*, 6(10):1-16. https://dx.doi.org/10.3389/fmicb.2015.00010

CARINO, A., MONTECILLO, A., ATIENZA, M.T.J., PATERNO, E., ILAG, L., FERNANDO, L. 2017. Phenotypic characterization and identification of *Lysinibacillus* sp. NBL1a capable of extracellular biogenic synthesis of gold nanoparticles. *Philipp Agric Sci*, 100: S81-S91.

CASTELLANE, T., OTOBONI, A., LEMOS, E. 2015. Characterization of exopolysaccharides produced by *Rhizobia* species. *R Bras Ci Solo*, 39(6): 1566-1575. https://dx.doi.org/10.1590/01000683rbcs20150084

CHAUDHARI, P., MASURKAR, S., SHIDORE, B., V, KAMBLE, SURESH. 2012. Effect of biosynthesized silver nanoparticles on *Staphylococcus aureus* biofilm quenching and prevention of biofilm formation. *Nano-Micro Lett* 4 (1): 34-39. https://doi.org/10.1049/iet-nbt.2011.0061

CHENG, F., BETTS, J.W., KELLY, S.M., SCHALLER, J., HEINZE, T. 2013. Synthesis and antibacterial effects of aqueous colloidal solutions of silver nanoparticles using aminocellulose as a combined reducing and capping reagent. *Green Chem.*, 15: 989–998. https://dx.doi.org/10.1039/C3GC36831A

CHHATRE, A., SOLASA, P., S,AKLE, S., THAOKAR, R., MEHRA, A. 2012. Color and surface plasmon effects in nanoparticles systems: Case of silver nanoparticles prepared by microemulsion route. *Colloids Surf A*, 404: 83-92. https://dx.doi.org/10.1016/j.colsurfa.2012.04.016

CHO, H.S., LEE, J.H., RYU, S.Y., JOO, S.W., CHO, M.H., LEE, J. 2013. Inhibition of *Pseudomonas aeruginosa* and *Escherichia coli* O157:H7 biofilm formation by plant metabolite ε–viniferin. *J Agric Food Chem*, 2013(61): 7120-7126. https://doi.org/10.1021/jf4009313

CIOFFI, N., RAI, M. (2012) Nano-antimicrobials: progress and prospects. Springer Science and Business Media, London

DOSSOUNON, Y.D., LEE, K., BELGHMI, K., BENZHA, F., BLAGHEN, M. 2016. Exopolysaccharide (EPS) production by *Exiguobacterium aurantiacum* isolated from Marchica lagoon ecosystem in Morocco. *Am J Microbiol Res*, 4(5): 147-152

DUBOIS, M., GILLES, K.A., HAMILTON, J.K., REBERS, P.A., SMITH, F. 1956. Colorimetric method for determination of sugars and related substances. *Anal Chem*, 28(3): 350-356. https://doi.org/10.1021/ac60111a017

DUNCAN, T.V. 2011. Applications of nanotechnology in food packaging and food safety: barrier materials, antimicrobials and sensors. *J Colloid Interface Sci* 363(1): 1–24. https://doi.org/10.1016/j.jcis.2011.07.017

EMTIAZI, G., ETHEMADIFAR, Z., HABIBI, M. 2004. Production of extra-cellular polymer in *Azobacter* and biosorption of metal by exopolymer. *Afri J Biotechnol*, 3(3): 330-333. https://doi.org/10.5897/ajb2004.000-2060

FREEMAN, D. J., FALKINER, F.R., KEANE, C.T. 1989. New method for detecting slime production by coagulase negative staphylococci. *J Clin Pathol*, 42, 872-874.

GE, L., LI, Q., WANG, M., OUYANG, J., LI, X., XING, M.M.Q. 2014. Nanosilver particles in medical applications: synthesis, performance, and toxicity. *Int J Nanomed*, 9(1): 2399–2407. https://doi.org/10.2147/ijn.s55015

GOMAA, E. 2016. Antimicrobial, antioxidant and antitumor activities of silver nanoparticles synthesized by *Allium cepa* extract: A green approach. *Gen Eng Biotechnol J*, 15(1). https://doi.org/10.1016/j.jgeb.2016.12.002

GROBBEN, G.J., SMITH, M.R., SIKKEM, J., DE BONT, J.A.M.1996. Influence of fructose and glucose on the production of exopolysaccharides and the activities of enzymes involved in the sugar metabolism and the synthesis of sugar nucleotides in *Lactobacillus delbrueckii* subsp. *Bulgaricus* NCFB 2772. *Appl Microbiol Biotechnol*, 46(3): 279–284. https://doi.org/10.1007/s002530050817

GURUNATHAN, S., KALISHWARALAL, K., VAIDYANATHAN, R., VENKATARAMAN, D., PANDIAN, S., MUNIYANDI, J., HARIHARAN, N., EOM, S. 2009. Biosynthesis, purification and characterization of silver nanoparticles using *Escherichia coli*. *Colloids Surf*, 74(1): 328-335. https://doi.org/10.1016/j.colsurfb.2009.07.048

GURUNATHAN, S., HAN, J.W., KWON, D.G., KIM, J.H. 2014. Enhanced antibacterial and anti-biofilm activities of silver nanoparticles against Gram-negative and Gram-positive bacteria. *Nanoscale Res Lett*, 9: 393. https://doi.org/10.1186/1556-276x-9-373

HEBEISH, A., HASHEM, M., ABD EL-HADY, M.M., SHARAF, S. 2012. Development of CMC hydrogels loaded with silver nano-particles for medical applications. *Carbohyd Polym*, 92: 407-413. https://doi.org/10.1016/j.carbpol.2012.08.094

IRAVANI, S., KORBEKANDI, H., MIRMOHAMMADI, S.V., ZOLFAGHARI, B. 2014. Synthesis of silver nanoparticles: chemical, physical, and biological methods. *Res Pharm Sci*, 9(6): 385-406

JIAN, W., ZHANG, L., SIU, K.C., SONG, A., WU, J.Y. 2016. Formation and physiochemical properties of silver nanoparticles with various exopolysaccharides of a medicinal fungus in aqueous solution. *Molecules,* 22(1):50. https://doi.org/10.3390/molecules22010050

KANMANI, P., LIM, S. 2013. Synthesis and structural characterization of silver nanoparticles using bacterial exopolysaccharide and its antimicrobial activity against food and multidrug-resistant pathogens. *Process Biochem*, 48(7): 1099-1106. https://doi.org/10.1016/j.procbio.2013.05.011

KALIMUTHU, K., BABU, R.S., VENKATARAMAN, D., BILAL, M., GURUNATHAN, S. 2008. Biosynthesis of silver nanocrystals by *Bacillus licheniformis*. *Colloids Surf B: Biointerface*, 65*:* 150-153. https://doi.org/10.1016/j.colsurfb.2008.02.018

KARBOWIAK, T., FERRET, E., DEBEAUFORT, F., VOILLEY, A., CAYOT, A. 2007. Investigation of water transfer across thin layer biopolymer films by infrared spectroscopy. *J Membr Sci*, 370:82-90. https://doi.org/10.1016/j.memsci.2010.12.037

KEMP, M.M., KUMAR, A., CLEMENT, D., AJAYAN, P., MOUSA, S., LINHARDT, R.J. 2009. Hyaluronan- and heparin-reduced silver nanoparticles with antimicrobial properties. *Nanomed (Lond)*, 4:421–429. https://doi.org/10.2217/nnm.09.24

KERSANI, I., ZADI-KARAM, H., KARAM, N. 2017. Screening of exopolysaccharide-producing coccal lactic acid bacteria isolated from camel milk and red meat of Algeria. *Afri J Biotechnol*, 16(18): 1078-1084. https://doi.org/10.5897/ajb2017.15907

KHANI, M., BAHRAMI, A., CHEGENI, A., GHAFARI, M.D., ZADEH, A.M. 2016. Optimization of carbon and nitrogen sources for extracellular polymeric substances production by *Chryseobacterium indologenes* MUT.2. *Iran J Biotech*, 14(2). https://doi.org/10.15171/ijb.1266

LANE, D.J. 1991. 16S/23S rRNA sequencing *In* E. Stackebrandt and M. Goodfellow (ed.) Nucleic acid techniques in bacterial systematics. John Wiley & Sons, New York. p. 115-175

LLAMAS, I., MATA, J., TALLON, R., BRESSOLLIER, P., URDACI, M., QUESADA, E., BÉJAR, V. 2010. Characterization of the exopolysaccharide produced by *Salipiger mucosus* A3T, a halophilic species belonging to the *Alpha proteobacteria*, isolated on the Spanish Mediterranean seaboard. *Mar Drugs*, 2010(8): 2240-2251. https://doi.org/10.3390/md8082240

LIANG, J., ZENG, F., ZHANG, M., PAN, Z., CHEN, Y., ZENG, Y., XU, Y., XU, Q., HUANG, Y. 2015. Green synthesis of hyaluronic acid-based silver nanoparticles and their enhanced delivery to CD44þ cancer cells. *RSC Adv*, 5:43733–43740*.* https://doi.org/10.1039/c5ra03083h

LI, J., LIN, Y., ZHAO, B. 2002. Spontaneous agglomeration of silver nanoparticles deposited on carbon film surface. *J Nanoparticle Res*, 4(4): 345-349

LOGARANJAN, K., RAIZA, A.J., GOPINATH, S.C.B., CHEN, Y. PANDIAN, K. 2016. Shape- and size-controlled synthesis of silver nanoparticles using *Aloe vera* plant extract and their antimicrobial activity. *Nanoscale Res Lett*, 11(520): 1-9. https://doi.org/10.1186/s11671-016-1725-x

LOO, C.Y., YOUNG, P.M., CAVALIERE, R., WHITCHURCH, C.B., LEE, W.H., ROHANIZADEH, R. 2013. Silver nanoparticles enhance *Pseudomonas aeruginosa* PAO1 biofilm detachment. *Drug Dev Ind Pharm,*40(6):719-29.

MARISELVAM, R., RANJITSINGH, A., NANTHINI, A.U., KALIRAJAN, K., PADMALATHA, C., SELVAKUMAR, P.M. 2014. Green synthesis of silver nanoparticles from the extract of the inflorescence of *Cocos nucifera* (Family: Arecaceae) for enhanced antibacterial activity. *Spectrochim Acta A Mol Biomol Spectrosc*, 129: 537-541. https://doi.org/10.1016/j.saa.2014.03.066

MASURKAR, SHALAKA, CHAUDHARI, PRATIK, SHIDORE, B., V, KAMBLE, SURESH. 2012. Effect of biosynthesized silver nanoparticles on *Staphylococcus aureus* biofilm quenching and prevention of biofilm formation. *IET nanobiotechnol / IET*, 6: 110-4. https://doi.org/10.1049/iet-nbt.2011.0061

MATSUKAWA, M., GREENBERG, E. 2004. Putative exopolysaccharide synthesis genes influence *Pseudomonas aeruginosa* biofilm development. *J Bacteriol,* 186(14):4449-56

MEHTA, A., SIDHU, C., PINNAKA, A., CHOUDHURY, A. 2014. Extracellular polysaccharide production by a novel osmotolerant marine strain of *Alteromonasmacleodii* and its application towards biomineralization of silver. *Plos One*, 9(6). https://doi.org/10.1371/journal.pone.0098798

MOHAN, S., OLUWAFEMI, O.S., SONGCA, S.P., JAYACHANDRAN, V.P., ROUXEL, D., JOUBERT, O., KALARIKKAL, N., THOMAS, S. 2016. Synthesis, antibacterial, cytotoxicity and sensing properties of starch-capped silver nanoparticles. *J Mol Liq,* 213:75–81. https://doi.org/10.1016/j.matpr.2015.08.023

MOHANTY, S., MISHRA, S., JENA, P., JACOB, B., SARKAR, B., SONAWANE, A. 2012. An investigation on the antibacterial, cytotoxic, and antibiofilm efficacy of starch-stabilized silver nanoparticles. *Nanomed Nanotechnol*, 8:916–924. https://doi.org/10.1016/j.nano.2011.11.007

MU'MINAH, BAHARUDDIN, HAZAMSUBAIR, FAHRUDDIN, BASODARWISAN. 2015. Isolation and screening of exopolysaccharide producing bacterial (EPS) from potato rhizosphere for soil aggregation. *Int J Curr Microbiol Appl Sci*, 4(6): 341-349. https://doi.org/10.1016/j.profoo.2015.01.007

MU, H., TANG, J., LIU, Q., SUN, C., WANG, T., DUAN, J. 2016. Potent antibacterial nanoparticles against biofilm and intracellular bacteria. *Sci Rep*, 6. https://doi.org/10.1038/srep18877

NICOLAUS, B., KAMBOUROVA, M., ONER, E.T. 2010. Exopolysaccharides from extremophiles: from fundamentals to biotechnology. *Environ Technol*, 31(10):1145-1158. https://doi.org/10.1080/09593330903552094

PEULEN, T.O., WILKINSON, K.J. 2011. Diffusion of nanoparticles in a biofilm. *Environ Scie Technol*, 45: 3367-3373. https://doi.org/10.1021/es103450g

PHANJOM, P., AHMED, G. 2017. Effect of different physicochemical conditions on the synthesis of silver nanoparticles using fungal filtrate of *Aspergillus oryzae* and their antibacterial effect. *Adv Nat Sci Nanosci Nanotechnol*, 8(4). https://doi.org/10.1088/2043-6254/aa92bc

RAJKUMARI, J., BUSI, S., VASU, A.C. 2017. Facile green synthesis of baicalein fabricated gold nanoparticles and their antibiofilm activity against *Pseudomonas aeruginosa* PAO1. *Microb Pathog*, 107: 261-269. https://doi.org/10.1016/j.micpath.2017.03.044

RAUWEL, P., KÜÜNAL, S., FERDOV, S., RAUWEL, E. 2015. A review on the green synthesis of silver nanoparticles and their morphologies studied via TEM. *Ad Mater Sci Eng*, 1-9. https://doi.org/10.1155/2015/682749

RAZACK, S.A., DURAIARASAN, S., MANI, V. 2016. Biosynthesis of silver nanoparticles and its application in cell wall disruption to release carbohydrate and lipid from *C. vulgaris* for biofuel production. *Biotechnol Rep*, 11:70-76. https://doi.org/10.1016/j.btre.2016.07.001

SABRI, M.A., UMER, A., AWAN, G.H., HASSAN, M.H., HASNAIN, A. 2016. Selection of suitable biological method for the synthesis of silver nanoparticles. *Sage J*, 6. https://doi.org/10.5772/62644

SANGHI, R., VERMA, P. 2009. Biomimetic synthesis and characterization of protein capped silver nanoparticles. *Bioresour Technol*, 100: 501-504. https://doi.org/10.1016/j.biortech.2008.05.048

SANYASI, S., MAJHI, R.K., KUMAR, S., MISHRA, M., GHOSH, A., SUAR, M., SATYAM, P., MOHOPATRA, H., GOSWAMI, C., GOSWAMII, L. 2016. Polysaccharide-capped silver nanoparticles inhibit biofilm formation and eliminate multidrug- resistant bacteria bydisrupting bacterial cytoskeleton with reduced cytotoxicity towards mammalian cells. *Sci Rep*, 6. https://doi.org/10.1038/srep24929

SARAVANAN, M., NANDA, A. 2010. Extracellular synthesis of silver bionanoparticles from *Aspergillus clavatus* and its antimicrobial activity against MRSA and MRSE. *Colloids Surf B*, 77(2):214–218. https://doi.org/10.1016/j.colsurfb.2010.01.026

SARAVANAN, C., RAJESH, R., KAVIARASAN, T., MUTHUKUMAR, K., KAVITAKE, D., SHETTY, P.H. 2017. Synthesis of silver nanoparticles using

bacterial exopolysaccharide and its application for degradation of azo-dyes. *Biotechnol Rep*, 15: 33-40. https://doi.org/10.1016/j.btre.2017.02.006

SATHIYANARAYANAN, G., BHATIA, S.K., KIM, H.J., KIM, J.H., JEON, J.M., KIM, Y.G., PARK, S.H., LEE, S.H., LEE, Y.K., YANG, Y.H. 2016. Metal removal and reduction potential of an exopolysaccharide produced by Arctic psychrotrophic bacterium *Pseudomonas* sp. PAMC 28620. *RSC Adv*, 6:96870–96881. https://doi.org/10.1039/c6ra17450g

SATO-BERRÚ, R., REDÓN, R., VÁZQUEZ-OLMOS, A., SANIGER, J.M. 2009. Silver nanoparticles synthesized by direct photoreduction of metal salts: Application in surface-enhanced Raman spectroscopy. *J Raman Spectrosc*, 40(4): 376–380. https://doi.org/10.1002/jrs.2135

SIRAJUNNISA, A.R., VELAYUTHAM, V., THANGAVELU, V. 2012. Medium optimization for the production of exopolysaccharide by *Bacillus subtilis* using synthetic sources and agro wastes. *Turkish J Biol* 37: 280-288

TAMBEKAR, D., DHUNDALE, V. 2012. Studies on the physiological and cultural diversity of bacilli characterized from Lonar lake (MS) India. *Biosci Discov*, 3(1): 34-39

TAMURA, K., NEI, M. 1993. Estimation of the number of nucleotide substitutions in the control region of mitochondrial DNA in humans and chimpanzees. *Mol Biol Evol*, 10:512-526. https://doi.org/10.1093/oxfordjournals.molbev.a040023

TIAGO, I., CHUNG, A.P., VERÍSSIMO, A. 2004. Bacterial diversity in a nonsaline alkaline environment: Heterotrophic aerobic populations. *Appl Environ Microbiol*, 73878-7387. https://doi.org/10.1128/aem.70.12.7378-7387.2004

VISHNUVARDHAN REDDY, S., THIRUMALA, M., FAROOQ, M. 2015. *Bacillus caseinilyticus* sp. nov. an alkali- and thermotolerant bacterium isolated from a soda lake. Int J Sys Evol Microbio 65: 2441–2446. https://doi.org/10.1099/ijs.0.000275

WEI, D., SUN, W., QIAN, W., YE, Y., MA, X. 2009. The synthesis of chitosan-based silver nanoparticles and their antibacterial activity. *Carbohyd Res*, 344:2375–2382. https://doi.org/10.1016/j.carres.2009.09.001

WELMAN, A., MADDOX, I., ARCHER, R. 2003. Screening and selection of exopolysaccharide-producing strains of *Lactobacillus delbrueckii* subsp. *bulgaricus*. *J Appl Microbiol*, 2003(95): 1200–1206. https://doi.org/10.1046/j.1365-2672.2003.02122.x

YUKSEKDAG, Z.N., ASLIM, B. 2008. Influence of different carbon sources on exopolysaccharide production by *Lactobacillus delbrueckii* subsp. *bulgaricus* (B3, G12) and *Streptococcus thermophilus* (W22). *Braz Arch Biol Technol*, 51(3): 581-585. https://doi.org/10.1590/s1516-89132008000300019